

City University of New York (CUNY)

CUNY Academic Works

Publications and Research

New York City College of Technology

2020

Simultaneous effects of rice husk silica and silicon carbide whiskers on the mechanical properties and morphology of sodium geopolymer

Akm Rahman

New York City College of Technology

Chirag Shah

New York University

Nihkil Gupta

New York University

[How does access to this work benefit you? Let us know!](#)

More information about this work at: https://academicworks.cuny.edu/ny_pubs/600

Discover additional works at: <https://academicworks.cuny.edu>

This work is made publicly available by the City University of New York (CUNY).

Contact: AcademicWorks@cuny.edu

Simultaneous effects of rice husk silica and silicon carbide whiskers on the mechanical properties and morphology of sodium geopolymer

Akm Samsur Rahman¹, Chirag Shah² and Nikhil Gupta²

Journal of Composite Materials
0(0) 1–10
© The Author(s) 2020
Article reuse guidelines:
sagepub.com/journals-permissions
DOI: 10.1177/0021998320928579
journals.sagepub.com/home/jcm



Abstract

The current research is focused on developing a geopolymer binder using rice husk ash–derived silica nanoparticles. Four types of rice husks were collected directly from various rice fields of Bangladesh in order to evaluate the pozzolanic activity and compatibility of the derived rice husk ashes with precursors of sodium-based geopolymers. Silicon carbide whiskers were introduced into sodium-based geopolymers in order to evaluate the response of silicon carbide whiskers to the interfacial bonding and strength of sodium-based geopolymers along with rice husk ashes. Compression, flexural and short beam shear tests were performed to investigate the synergistic effect of rice husk ashes–derived silica and commercially available silicon carbide whiskers. Results show that rice husk ashes–derived spherical silica nanoparticles reduced nano-porosity of the geopolymers by ~20% and doubled the compressive strength. The simultaneous additions of rice husk ashes and silicon carbide whiskers resulted in flexural strength improvement by ~27% and ~97%, respectively. The increase in compressive strength due to the inclusion of silica nanoparticles is related to the reduction in porosity. The increase in flexural strength due to simultaneous inclusion of silica and silicon carbide whiskers suggest that silica particles are compatible with the metakaolin-based geopolymers, which is effective in consolidation. Finally, microscopy suggest that silicon carbide whiskers are effective in increasing bridged network and crack resistance.

Keywords

Rice husk ash, whiskers, metakaolin, geopolymer, crack bridging; dispersion strengthening, fire resistance, cementitious composite

Introduction

The worldwide growing demand of rice has raised a deep concern about disposal of non-bio-degradable rice husk. The global rice demand is estimated to be 700 Million Tons in the present year 2020. Rice husk makes up approximately 20% of the total rice production. For many rice-producing countries, the most common applications of rice husk are thermal power plants and charcoals for household cook stoves. However, rice husk is a proven source of pure amorphous silica,^{1,2} which is an important ingredient of geopolymer.³ The current research focused on the novel conversion of rice husk to geopolymers for application in composite materials.

Geopolymer is an aluminosilicate binder formed by alkaline activation of solid alumina and silica containing precursor materials at or slightly above room

temperature.⁴ Although this geopolymer technology has been studied widely, its applications have not been widespread for the technical and non-technical reasons.^{5,6} The term geopolymer was introduced in the 1970s by Davidovits to describe a family of alkali-activated aluminosilicate binders, and later became

¹Mechanical Engineering, New York City College of Technology, City University of New York, USA

²Composite Materials and Mechanics Laboratory, Department of Mechanical and Aerospace Engineering, Tandon School of Engineering, New York University, Brooklyn, NY 11201, USA

Corresponding author:

Akm Samsur Rahman, New York City College of Technology, 186 Jay St Brooklyn, NY, New York 11201-2983, USA.

Email: asrahman@citytech.cuny.edu

popular to describe a larger variety of alkali-activated binders.⁷

Geopolymers are composed of tetrahedral silicate and aluminate units linked in a three-dimensional structure by covalent bonds, with the negative charges associated with tetrahedral aluminum charge-balanced by alkali cations. The raw materials include two parts: reactive aluminosilicate solids, such as fly ash and calcined clays, and an alkaline activating solution, usually an alkali metal hydroxide or silicate solution.⁴ Several sources for Geopolymer ingredients are presented in Figure 1.

The critical roles in the geopolymerization are thought to be played by alkali activation of fly ash in an alkaline solution. The chains in aluminosilicate oligomers can be in the form of polysialate -Al-O-Si-chain, polysialate siloxo -Al-O-Si-Si- chain and polysialate disiloxo -Al-O-Si-Si-Si- chain, depending upon the Si/Al ratio.⁹ In aluminosilicate monomers, Si⁴⁺ is partially substituted by Al³⁺ and the resultant negative charge in the aluminosilicate chains is balanced by alkali cations such as Na⁺ or K⁺.¹⁰ The Si/Al ratio significantly impacts the final structure of the resulting geopolymer¹¹ and has a remarkable effect on the porosity, which is one of the most important factors in governing the mechanical performance of geopolymer.¹²

In addition to the Si/Al ratio, the microstructure of fly ash-based geopolymer is strongly affected by the alkaline solution. When fly ash comes in contact with alkali (e.g. NaOH, KOH), Si⁴⁺, Al³⁺ and other ions start to be released. The amount of released Si⁴⁺ and Al³⁺ is influenced by the concentration of NaOH solution. NaOH solution of high concentration (10 mol/L) is beneficial for decomposing aluminosilicate in the fly ash and then release Si⁴⁺ and Al³⁺.¹³ Moreover, the transfer of Al³⁺ and Si⁴⁺ species and the poly-condensation of aluminosilicate oligomers can also be accelerated by an alkaline solution with high concentration.¹⁴ Furthermore, charge density and nucleation of aluminosilicate chains depend on the types of alkaline cations, which affect the rate and the extent of polymerization.¹⁵

Alkaline cations also serve as a structure-directing agent in the geopolymerization. The leaching rates of Si⁴⁺ and Al³⁺ decide the actual available Si/Al ratio in a series of reactions to form geopolymer and subsequently play a pivotal role in the structure of fly ash-based geopolymer. A recent study revealed that the addition of Na₂SiO₃ to alkali solution can increase the Si/Al ratio, resulting in a lower porosity and a finer pore system of geopolymer matrix.¹⁶ The activation procedure also influences the compressive strength of fly ash-based geopolymer. For the current study, KOH was used for the alkali activation of the geopolymer. The K⁺ cation is larger in size in comparison to Na⁺, which leads to lower surface charge density and higher degree of polymerization.¹⁷ However, at room temperature, the dissolution of fly ash is not completed and requires further curing.¹⁸ Curing allows the cross-linking of the polymer chains, thus forming rigid cross-linked aluminosilicate (poly-sialate) bonds, which govern the overall properties of the geopolymer panel. Curing at high temperatures increases the compressive strength by removing water from the fresh geopolymer, causing the collapse of the capillary pores with a denser structure.¹⁹ Geopolymers can be cured at the room temperature but the compressive strength of high temperature cured resins is higher.²⁰ Geopolymer curing can occur between room temperatures and 100°C with little CO₂ emission.^{21,22}

Calcined rice husk, also called rice husk ash (RHA), is very rich in amorphous silica, which exhibits high reactivity. Due to the stored thermal energy, these highly reactive materials can readily make strong bonds with aluminosilicate during geopolymerization process. Several studies²³⁻²⁵ have demonstrated the development of geopolymer using RHA with an interest in developing alternative cementitious materials for structural applications. Those studies have reported RHA-based geopolymer as a blessing to the environment since it recycles bio-waste, lowers greenhouse gas emission and reduces processing temperature. However, detailed studies focused on geopolymer-based continuous fiber reinforced composites for high-temperature applications are still lacking. The potential of RHA



Figure 1. Binders for the geopolymer production.⁸

from south east Asian countries in geopolymer is also unknown, where rice is a major edible product. Additions of RHA in the matrix of fiber reinforced geopolymer composites can make them eco-friendly and also improve their mechanical performance.

Sodium-based ingredients have been widely implemented in geopolymer formulations.^{26–30} Studies have shown that sodium-based geopolymers offer higher setting time compared to potassium-hydroxide-based systems, which is advantageous in handling³⁰ because formation of complex shapes require higher time. Several studies on geopolymer-based composites^{21,31} suggest that high-aspect ratio nanofillers are effective in toughening and strengthening of continuous fiber reinforced geopolymer composites. Nanofiller length, strength and reinforcing capabilities are deemed necessary parameters in toughening. However, the mechanism involved in toughening of geopolymer using nanofibers is still unclear.

Therefore, the current study is focused on investigating the synergistic effect of RHA and SiC whiskers on the performance of geopolymer solids in order to develop high-performance eco-friendly composite materials. This research is focused at recycling efforts on two types of solid wastes into a single stream application. Processing of those wastes otherwise would be susceptible to larger greenhouse emissions; the current processing and treatment is beneficial to the environment.

Experimental procedure

Materials of the experimentation

Metakaolin, the main ingredient of geopolymer, was prepared from PLUS white kaolin (Supplied by Charles B. Chrystal Co., Inc). The main ingredients of kaolin are silicon dioxide (SiO_2) (44.5 wt%), Al_2O_3 (39.4 wt%) and loss on ignition components (15 wt%). Sodium silicate ($\text{Na}_2\text{SiO}_3 \cdot 9\text{H}_2\text{O}$, ~40 wt%) solution was purchased from Carolina Biological supply company. Dry sodium hydroxide pallets were collected from Carolin Biological Inc. (Item #889460). Silicon carbide whiskers (SCW) were supplied by Pyromeral Inc. The trade name of SCW is Silar SC9M and its manufacturer is Advanced Composite Materials. These are de-agglomerated and very high-modulus rigid nanofibers. The reported length of the fibers is in the range 10–12 μm ; however, scanning electron microscope (SEM) observations showed that most of the fibers were 25–30 μm in length.

Synthesis of RHA silica

Four types of RHs were collected directly from rice fields of the different parts of Bangladesh. According to local supplier those are B-11, B-28, B-29 and

SARNA. RHs were first washed overnight in 30% nitric acid to dissolve some chemicals and impurities. Nitric acid was decanted and the RH was washed three times using distilled water followed by drying. The cleaned and dried Sarna and B-11 RH is shown in Figure 2(a) and (b). The dried husks were calcined in a furnace in air atmospheric at 650°C for 7 h. The residual rice husk or RHA was then collected from the oven, washed again in 30% nitric acid and water and then dried. Then, RHA was crushed and stored for use as the filler in the geopolymer.

Metakaolin synthesis

Primary ingredient of the proposed geopolymer is metakaolin or calcined kaolinite. Metakaolin transformation from kaolin is accomplished by calcination process upon heating in the range 500–750°C for 2–10 h.³² Calcination results in the removal of water and hydroxyl (OH^-) groups associated with Al-O-H bonds of kaolin, which increases the reactivity and pozzolanic energy of metakaolin. Surface hydroxyl groups break away easier than the hydroxyl groups within the material because of longer bond length on the surface.²¹ This pozzolanic nature of metakaolin is essential for self-activation in the alkaline medium by reacting with other geopolymer ingredients, alkali silicate and reactive silica in particular.^{33,34} Metakaolin prepared using the PLUS white kaolin (supplied by Charles B. Crystal Co. Inc.) was heated at 750°C for 5 h in air atmosphere to obtain metakaolin MK-750.

Synthesis of geopolymer

Sodium-based geopolymer (Na-GP) was prepared using sodium silicate supplied by Carolina Biological Inc. First, dry sodium silicate and metakaolin powder were mixed in 8 M NaOH with a mole ratio of $\text{Na}_2\text{O}/\text{Al}_2\text{O}_3 = 1.64$, $\text{SiO}_2/\text{Al}_2\text{O}_3 = 3$, $\text{H}_2\text{O}/\text{Na}_2\text{O} = 9.3$, $\text{Na}_2\text{O}/\text{SiO}_2 = 0.55$. Manual stirring was followed by mixing in an ARM 310 Thinky mixer at 2000 r/min. Between each 30 s mixing cycles, the resultant slurry was stored in a freezer for few minutes to remove heat. The first step of curing was performed at 80°C in a sealed environment to ensure that moisture was retained, not allowing the specimens to prematurely dry. Subsequently, the test specimens were dried and heat treated at 150°C and 350°C, respectively, according to the test matrix shown in Table 1. The specimens were tested once they were cooled down to room temperature after the heat treatment.

Synthesis of RHA and whisker reinforced geopolymer

Nanomaterial reinforced geopolymer was prepared using 4 wt% RHA and 4 wt% SCW according

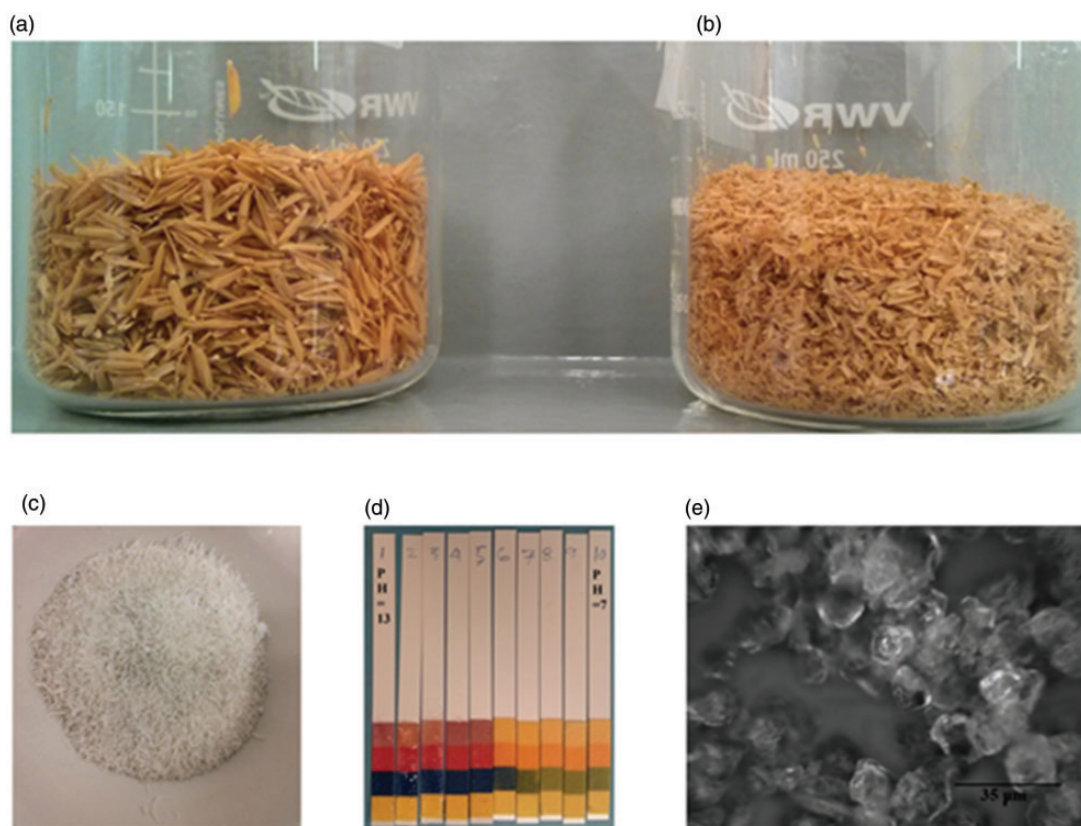


Figure 2. (a) Acid washed (a) RH-Sarna, (b) RH-B-II, (c) RHA after calcination at 650°C in air for 7 h, (d) transformation of basic to neutral pH during the silica extraction reaction and (e) particles of the silica extracted from RHA. RHA: rice husk ash.

Table 1. Test matrix of geopolymer with the variations in RHA and SCW and treatment temperatures.

Material	Compression test			Flexural test 350°C	Shear test 350°C
	80°C	150°C	350°C		
Neat resin	+	+	+	+	
Neat + 4 wt% RHA	+	+	+	+	+
Neat + 4 wt% RHA + 4 w% SCW	+	+	+	+	+

RHA: rice husk ash; SCW: silicon carbide whiskers.

to the composition shown in Table 1. An early study suggested that a gradual increase in SCW reinforcement to 2 wt% resulted in a linear increase in fracture toughness of geopolymer by 113%.⁴ This benchmark study created an opportunity to conduct the current study with nanomaterial at a safe level, 4 wt% for example. Nanoparticle mixing and sample preparation were conducted using a procedure similar to the neat geopolymer sample preparation.

Characterization techniques

Compressive strength was measured using an Applied Test Systems, Inc. electromechanical load frame. The tests were performed by placing the specimens of nominal dimensions of 17 mm length and 6 mm diameter in an aluminum compression cage and compressing at a crosshead displacement rate of 0.5 mm/min (0.02 in/min) as per ASTM C 1424 standard.³⁵ At least five specimens were tested for each material type.

The un-notched beam flexure and short beam shear tests were performed³⁶ and the flexural strength was calculated by

$$S_b = \frac{3FL}{2bw^2} \quad (1)$$

where, S_b = flexural strength, F = breaking load, L = span length, b = specimen width and w = specimen thickness. In order to validate the fracture toughness results, the beam depth and width in both tests were kept constant. The L/w ratio for flexural and short beam shear tests were kept at 16 and 4, respectively.

Thermogravimetry analysis (TGA) was used to evaluate the degradation of RH during the thermal treatment. The purpose of this study was to correlate the weight losses with physicochemical transformations of RH at different stages of calcination process. A Seiko I SSC/5200 TG/DTA 220 (by Seiko Instruments Inc.) was used for this analysis. This instrument measures mass change between the sample and the reference and thus enables the equipment to function as both thermogravimetry and differential thermal analyzer (DTA) simultaneously. DTA results were obtained from the difference in temperatures between the sample and the reference. All specimens were tested in aluminum pan under 20–30 mL/min of nitrogen flow using about 20–25 mg of crushed specimen.

Elemental analysis of RHA was performed using EDX analyzer. Elemental composition of RHA was then compared with stoichiometric SiO_2 . Microstructural image analysis of RHA was performed to understand the size of silica particles. A suspension of RHA was prepared in ethanol using ultrasonic horn. Then a small drop of the suspension was allowed to dry on a glass slide, which was inspected using an Optimus optical microscope.

X-ray diffraction (XRD) of RHA was performed using Scintag X-2 X-ray powder diffractometer. The 0.1542 nm wavelength Cu-K α radiation was used and the specimens were scanned in 5 to 85° range with a step size of 0.02°.

Measurement of open porosities is an effective tool for understanding the level of consolidation of the material. Apparent open porosity of the specimen is measured in terms of water absorption, which was performed by measuring the weight difference (in air) of completely dry specimens (heated at 150°C) before and after submerging into water as per ASTM C-20-2010 standard.^{37,38} The porosity is calculated by

$$P(\%) = [1 - ((W_D - W_S)/\rho_w)/V_T] \times 100 \quad (2)$$

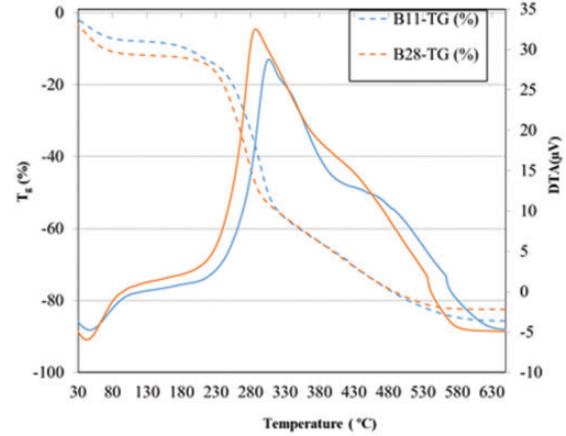


Figure 3. T_g and DTA of rice husk B-11 and B-28. DTA: differential thermal analyzer; RHA: rice husk ash.

where, W_D is dry mass of the specimen (g), W_S is submerged mass of the specimen (g), ρ_w is the density of water (g/cm^3) and V_T is the total volume of the specimen. W_S was measured using Archimedes principle.³⁹

Results and discussion

Thermal analysis of RHA

Thermal degradation of two RH specimens, B11 and B28, are presented in Figure 3. Both RH samples were investigated under 20–30 mL/h nitrogen flow up to 650°C. During the thermal treatment of both specimens, 85% of initial weights have been lost, which represents organic volatile compound content. These peaks indicate the ability of RH to produce thermal energy due to high-temperature combustion. In summary, the unburnt 15 wt% amount is considered as RHA, which is expected to be silica-rich materials. Major weight loss occurred in 180–480°C temperature range, which indicated reduction of organic volatile compounds such as starch, lignin, cellulose and hemicellulose.⁴⁰ As seen from the DTA curves, this weight loss can be further broken down in two parts, of which second major loss of 60 wt% is associated with breakdown of cellulose constituents to combustible volatiles, water, carbon dioxide and char.⁴¹ Thermal degradation continues until ~600°C. At this temperature, 15–20 wt% material was left as residue, which is called RHA, a fully converted silica.

Elemental and phase analysis of RHA

Elemental weight percentages of RHA were estimated using EDS spectrum in Figure 4. It is found that more than 80 wt% of the composition constitutes only silica and oxygen and their relative magnitudes represents a

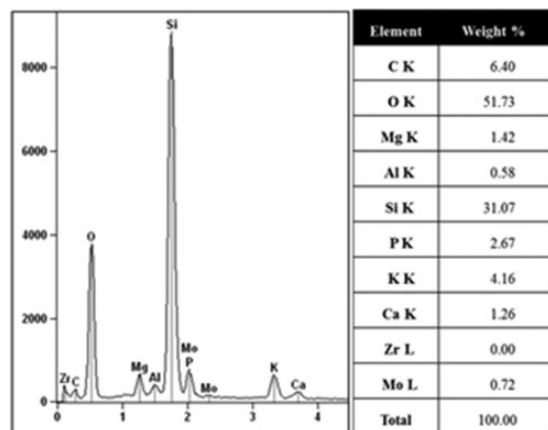


Figure 4. EDS spectrum and elements of RHA B-28 (at 4.5 kV). RHA: rice husk ash.

close approximation of stoichiometric silica (SiO_2) (% At. Si = 31.05 and O = 51.73).⁴² A small amount of carbon (6.4 wt%) in the RHA may represent unburned carbon content from RH. Since the TGA was conducted in nitrogen atmosphere, carbon content is not unexpected. This result indicates that in order to obtain a stoichiometric silica compound, this carbon content is needed to calcine at temperature above 650°C and higher oxygen concentration. Once the calcination process is completed, pure Si is left at this high temperature, which continues to react with oxygen, forming SiO_2 . Due to intrinsic nature of RHA-derived silicon, a finely divided SiO_2 is formed during this calcination process, which exhibits a unique pozzolanic nature when mixed with geopolymer in the presence of an alkaline medium.⁴³ Figure 5(a) and (b) represents those particles of SiO_2 derived from RH.

Figure 6 presents XRD patterns of four types of RHAs evaluated in this study. A diffused wide peak was found in all RHA specimens centered at $2\theta = 22.5^\circ$. This represents the presence of amorphous SiO_2 or disordered cristobalite. Similar diffused peaks were observed by Genieva et al.⁴⁰ in their XRD analysis of pyrolyzed RHA. The peak was also matched with Aerosil 200 fumed silica, which is nonporous and highly dispersed.⁴⁴

XRD analysis of B-28 and B-11 shows crystalline peaks at around $2\theta = 26.5^\circ$, which suggests the presence of quartz. It is reported that crystalline nature indicates lower reactivity, while amorphous nature indicates higher reactivity.^{45,46} A higher reactivity results in a higher rate of diffusion and lower effectiveness as a reinforcement. Thus, the balance between pozzolanic reactivity and reinforcement ability is essential for RHA in geopolymerization process. Therefore, the comparison of the reinforcing capability of B-11 and Sarna at $\sim 650^\circ\text{C}$ would be of interest to explore.

Effect of SiO_2 additions in porosity of geopolymer

Figure 7 presents the effect of RHA on the porosities of geopolymer at 300°C . With only 4 wt% RHA addition, 20–25% porosity of geopolymer dropped down to 7 to 12%. Nonetheless, this porosity is higher than sintered ceramics such as Al_2O_3 and SiN ; however, this may be a suitable route to reduce porosity and densify non-sintered ceramics.

Flexural and shear strength variations with nanofillers

Flexural and shear strengths of neat, RH-derived SiO_2 and SCW reinforced geopolymer are presented in Figure 8(a). It is found that SiO_2 and SCW addition increased both types of strength. The SiO_2 + SCW addition increased the flexural and shear strengths by 97% and 158%, respectively. However, only SiO_2 addition did not show any significant increase in both type of strengths. Since flexure and shear strengths depend on the ability to resist tensile failure and sliding frictions, high-aspect ratio nanofillers such as SiC whiskers are capable of improving these properties by crack-bridging mechanism. As expected, SiO_2 nanoparticles did not show any bridging, however they filled the process-related nano-porosities of the geopolymer matrix, resulting in decrease in the number of defects. Conversely, SiC whiskers have stoichiometric surface with larger Si atom residing outside and smaller carbon atom sitting in the interstitial space. This unique characteristic of SiC whisker not only allows a strong bonding with geopolymer precursor it also retains its chemical and thermal resistance in the geopolymer matrix. Therefore, the combination of RH-based SiO_2 and SiC whiskers is effective as a reinforcement, where the former reduces the porosity and the later increases the crack bridging and sliding frictions between the layers of metakaolin sheets.⁴⁷

Load-displacement curves are presented in Figure 8(b) for neat and nanofilled geopolymer treated at 150°C and 350°C . It is found that the loading rate (load per unit deflection) of neat geopolymer increased with the post-processing temperature. The loading rate further increased (13,000 lb/in vs 13,871 lb/in) with the addition of RHA and SiC whisker.

Microscopic evaluations of nanofilled geopolymer

SEM images of fracture surface of neat and RHA silica reinforced geopolymer is shown in Figure 9(a) and (b). Also, fracture surfaces of SCW reinforced geopolymer are shown in Figure 9(c) and (e). Figure 9(c) presents overall distribution of SCW in the geopolymer matrix. Figure 9(a) presents a clean fracture surface of neat GP, which is an indication of low energy release state.

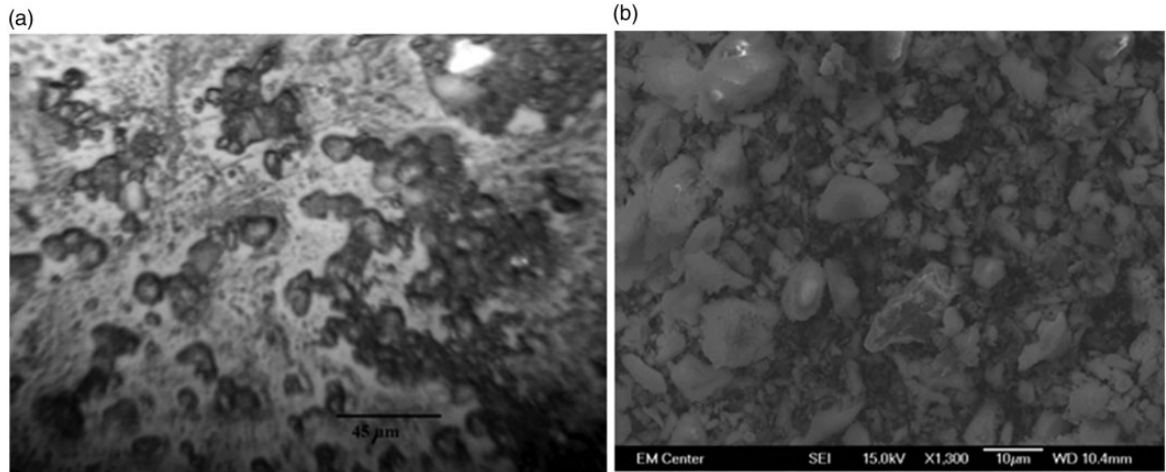


Figure 5. (a) Microscopic view RHA B-28 (average particle size 12 μm) and (b) at $\times 1300$ magnification. RHA: rice husk ash.

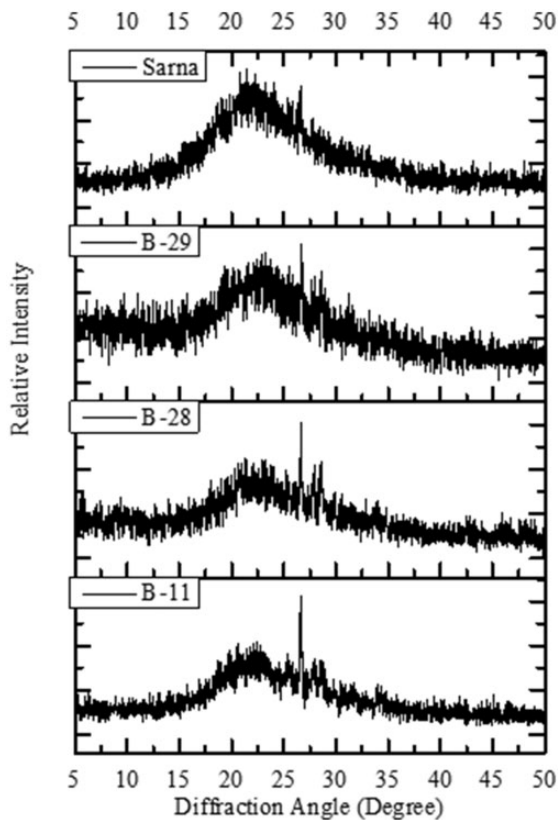


Figure 6. X-ray diffraction analysis of four different types of RHA (Sarna, B-29, B-28 and B-11). RHA: rice husk ash.

Figure 9(b) shows RHA silica particles on the fracture surface and its state of bonding with GP. It represents relatively rough surface and state of moderately high energy release rate. Figure 9(d) indicates that the diameter of the embedded SCW is about $0.6\mu\text{m}$. From Figure 9(e) it is seen that SCWs are well bonded with geopolymer. No interfacial separation between SCW

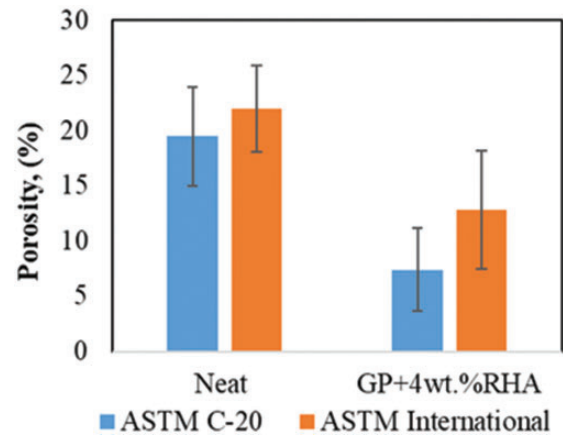


Figure 7. Apparent porosities of geopolymer with and without 4 wt% RHA measured by two methods. RHA: rice husk ash.

and geopolymer is revealed in this image. SCW is alkali-resistant and revealed as a separate phase from geopolymer, marked as Na-GP. SCW failed across the thickness, which suggests that SCW creates a crack-bridging effect and increases the shear resistance. Similar observations have been found elsewhere.^{4,48}

Summary

This study evaluated micro-structural and crystalline nature of RH collected from various zones of Bangladesh. This study demonstrated the growth mechanism of pure SiO_2 and the origination of pozzolanic nature that assisted the RH-derived SiO_2 into the formation of strong bonding with metakaolin. Addition of this SiO_2 demonstrated a $\sim 23\text{--}35\%$ increase in both flexural and short beam shear strength of metakaolin-based geopolymer. Addition of SCWs has shown

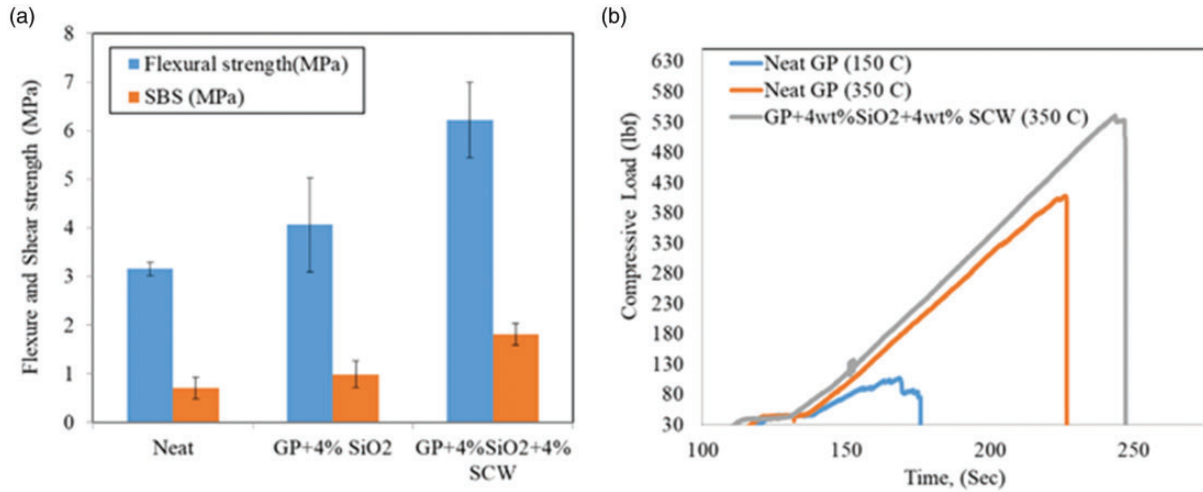


Figure 8. (a) Variations in flexural and shear strengths with the additions of SiO₂ and SCW and (b) compressive loading rates of neat and nano-reinforced geopolymer. SCW: silicon carbide whiskers.

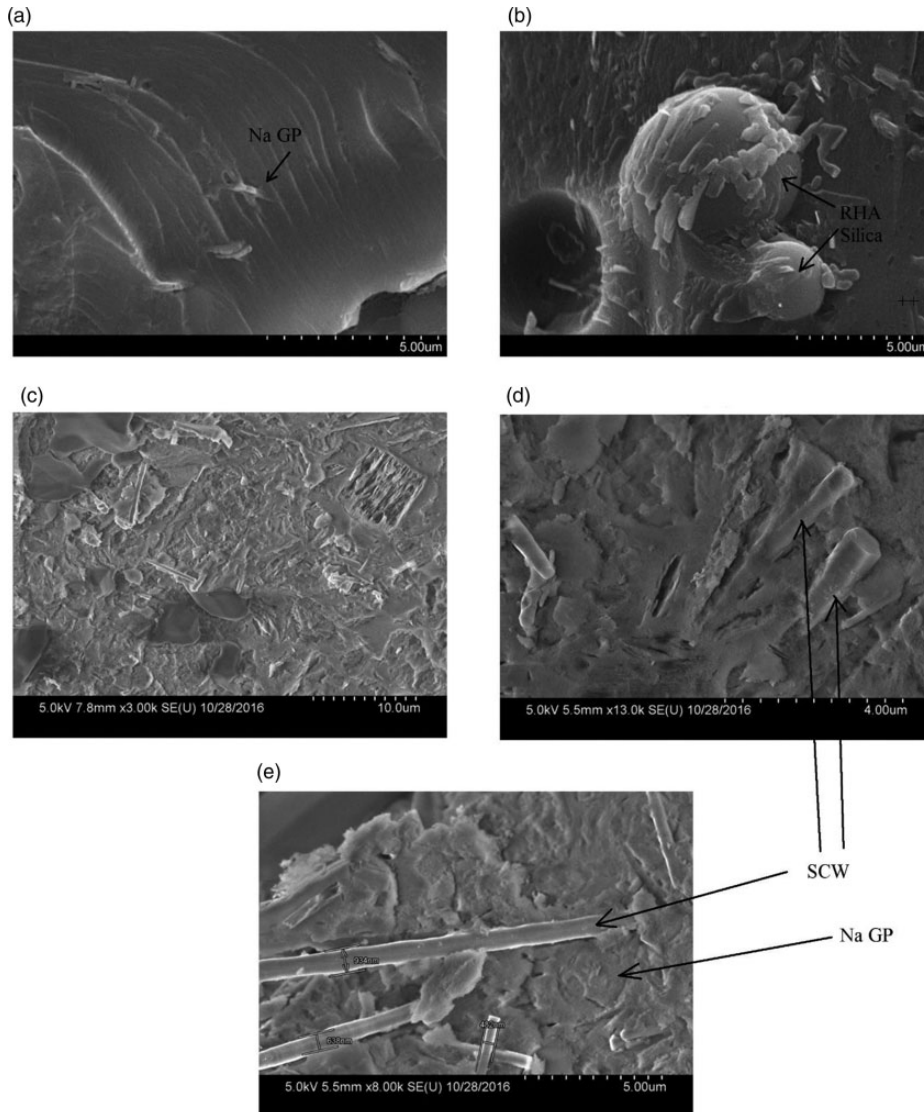


Figure 9. Fracture surface of (a) neat Na-GP (b) RHA silica-reinforced GP and (c-e) RHA silica + SCW reinforced GP at various magnifications. Na-GP: sodium-based geopolymer; RHA: rice husk ash; SCW: silicon carbide whiskers.

respective 97% and 158% increases in flexural and shear strengths. SiC provides naturally expected performance due to the reduced free-carbon and stoichiometric surface chemistry. This unique surface chemistry resulted in a separate phase of SCW in the geopolymer matrix which supported crack-bridging effect under thermomechanical stress. The resultant geopolymer formulations are potentially suitable for waste reduction and development of green cementitious composites for structural applications.

Acknowledgment

The first author acknowledges Composite and Biomaterials Lab at New York City College of Technology of the City University of New York.

Declaration of Conflicting Interests

The author(s) declared no potential conflicts of interest with respect to the research, authorship, and/or publication of this article.

Funding

The author(s) received no financial support for the research, authorship, and/or publication of this article.

References

1. Le VH, Thuc CNH and Thuc HH. Synthesis of silica nanoparticles from Vietnamese rice husk by sol-gel method. *Nanoscale Res Lett* 2013; 8: 58.
2. Lima SPBde, et al. Production of silica gel from residual rice husk ash. *Química Nova* 2011; 34: 71–75.
3. Chandani T, et al. Influence and role of feedstock Si and Al content in geopolymer synthesis. *J Sustain Cement-Based Mater* 2015; 4: 129–139.
4. Rahman AS, Jackson P and Radford DW. Improved toughness and delamination resistance in continuous fiber reinforced geopolymer composites via incorporation of nano-fillers. *Cement Concr Compos* 2020; 108: 103496.
5. Zhang Z, Provis JL, Reid A, et al. Geopolymer foam concrete: An emerging material for sustainable construction. *Constr Build Mater* 2014; 56: 113–127.
6. van Deventer JSJ, Provis JL, Duxson P, et al. Chemical research and climate change as drivers in the commercial adoption of alkali activated materials. *Waste Biomass Valor* 2010; 1: 145–155.
7. Davidovits J. *Geopolymer chemistry and applications*. Saint-Quentin, France: Institut Géopolymère; 2008.
8. Aldin Z. *3D Printing of geopolymer concrete*. Master's Thesis, Delft University of Technology, the Netherlands, 2019.
9. Zhuang XY, Chen L, Komarneni S, et al. 2016. *Fly ash-based geopolymer: Clean production, properties and applications*. *J Clean Prod* 2016; 125: 253–267.
10. Davidovits J. 30 years of successes and failures in geopolymer applications, market trends and potential breakthroughs. In: *Geopolymer 2002 conference*, Saint-Quentin (France), Melbourne (Australia), Geopolymer Institute, 2002.
11. He J, Zhang J, Yu Y, et al. The strength and microstructure of two geopolymers derived from metakaolin and red mud fly ash admixture: A comparative study. *Constr Build Mater* 2012; 30: 80–91.
12. Kriven WM, Bell JL and Gordon M. Microstructure and microchemistry of fully reacted geopolymers and geopolymer matrix composites. *Ceram Trans* 2003; 153: 227–250.
13. Xu H and van Deventer JSJ. The geopolymerisation of natural aluminosilicates. In: *Proceedings of the 2nd international conference on geopolymer*, France, 1999, pp.43–63.
14. Lizcano M, Hyunsoo K, Basu S, et al. Mechanical properties of sodium and potassium activated metakaolin-based geopolymers. *J Mater Sci* 2011; 47: 2607–2616.
15. Duxson P, Lukey GC, Separovic F, et al. Effect of alkali cations on aluminum incorporation in geopolymeric gels. *Ind Eng Chem Res* 2005; 44: 832–839.
16. Ma Y, Hu J and Ya G. The pore structure and permeability of alkali activated fly ash. *Fuel* 2013; 104: 771–780.
17. van Jaarsveld JGS and van Deventer JSJ. Effect of the alkali metal activator on the properties of fly ash-based geopolymer. *Ind Eng Chem Res* 1999; 38: 3932–3941.
18. Chen C, Gong W, Lutze W, et al. Kinetics of fly ash leaching in strongly alkaline solutions. *J Mater Sci* 2011; 46: 590–597.
19. Leung CKY and Pheerapha T. Very high early strength of microwave cured concrete. *Cem Concr Res* 1995; 25: 136–146.
20. Somna K, Jaturapitakkul C, Kajitvichyanukul P, et al. NaOH activated ground fly ash geopolymer cured at ambient temperature. *Fuel* 2011; 90: 2118–2124.
21. Rahman AKM. *Nanofiber reinforcement of a geopolymer matrix for improved composite materials mechanical performance*. Dissertation, Colorado State University, 2015.
22. Davidovits J. Geopolymers inorganic polymeric new materials. *J Therm Anal Calorim* 1991; 37: 1633–1656.
23. Thakur RN and Ghosh S. Effect of mix composition on compressive strength and microstructure of fly ash based Geopolymer composites. *J Eng Appl Sci* 2009; 4: 68–74.
24. Wansom S, Janjaturaphan S and Sinthupinyo S. Characterizing pozzolanic activity of rice husk ash by impedance spectroscopy. *Cem Concr Res* 2010; 40: 1714–1722.
25. Bhuvaneshwari B, Sasmal S, Baskaran T, et al. Role of nano oxides for improving cementitious building materials. *J Civil Eng Sci* 2012; 1: 52–58.
26. Patankar SV, Ghugal YM and Jamkar SS. Effect of concentration of sodium hydroxide and degree of heat curing on fly ash-based geopolymer mortar. *Ind J Mater Sci* 2014; 2014.
27. Musil SS, Keane PF and Kriven WM. Green composite: Sodium-based geopolymer reinforced with chemically extracted corn husk fibers. In: *Developments in strategic materials and computational design IV – A collection of papers presented at the 37th international conference on*

- advanced ceramics and composites, ICACC 2013*. 10th ed. 2014, pp.123-133.
28. Cwirzen A, et al. The effect of limestone on sodium hydroxide-activated metakaolin-based geopolymers. *Constr Build Mater* 2014; 66: 53–62.
 29. Shaikh FUA and Vimonsatit S. Compressive strength of fly-ash-based geopolymer concrete at elevated temperatures. *Fire Mater* 2015; 39: 174–188.
 30. Sabitha D, et al. Reactivity, workability and strength of potassium versus sodium-activated high volume fly ash-based geopolymers. *Curr Sci* 2012; 103: 1320–1327.
 31. Rill E, Lowry DR and Kriven WM. Properties of basalt fiber reinforced geopolymer composites. In: *Strategic materials and computational design – A collection of papers presented at the 34th international conference on advanced ceramics and composites*. 10th ed., 2010, Vol. 31, pp.57-67.
 32. Zhang ZH, Yao X, Zhu H, et al. Activating process of geopolymer source material: Kaolinite. *J Wuhan Univ Technol-Mat Sci Ed* 2009; 24: 132–136.
 33. Provis JL. *Modelling the formation of geopolymers*. PhD Dissertation, The University of Melbourne, Australia, 2006.
 34. Ribeiro RA Sá, Sá Ribeiro MG and Kriven WM. A Review of particle-and fiber-reinforced metakaolin-based geopolymer composites. *J Ceramic Sci Technol* 2017; 8: 307–322.
 35. ASTM C1424-2004. *Standard test method for monotonic compressive strength of advanced ceramics at ambient temperature*. West Conshohocken, PA: ASTM International, 2004.
 36. ASTM C 1161-08. *Standard test method for flexural strength of advanced ceramics at ambient temperature*. West Conshohocken, PA: ASTM International, 2010.
 37. ASTM C20-00-2010. *Standard test methods for apparent porosity, water absorption, apparent specific gravity, and bulk density of burned refractory brick and shapes by boiling water*. West Conshohocken, PA: ASTM International, 2010.
 38. Montes F, Valavala S and Haselbach L. A new test method for porosity measurements of Portland cement pervious concrete. *J ASTM Int* 2005; 2: 1–13.
 39. <https://www.britannica.com/science/Archimedes-principle>(accessed 26 January 2019).
 40. Genieva S, et al. Characterization of rice husks and the products of its thermal degradation in air or nitrogen atmosphere. *J Thermal Anal Calorimetr* 2008; 93: 387–396.
 41. Stefani PM, et al. Thermogravimetric analysis of composites obtained from sintering of rice husk-scrap tire mixtures. *J Thermal Anal Calorimetr* 2005; 81: 315–320.
 42. Akl MA, et al. Preparation and characterization of silica nanoparticles by wet mechanical attrition of white and yellow sand. *J Nanomed Manotechnol* 2013; 4: 183–200.
 43. Davraz M and Gunduz L. Engineering properties of amorphous silica as a new natural pozzolan for use in concrete. *Cement Concr Res* 2005; 35: 1251–1261.
 44. <https://www.aerosil.com/product/aerosil/downloads/technical-overview-aerosil-fumed-silica-en.pdf> (accessed 27 January 2019).
 45. Chandrasekhar S, et al. Review processing, properties and applications of reactive silica from rice husk—an overview. *J Mater Sci* 2003; 38: 3159–3168.
 46. Fernandes IJ, et al. Characterization of silica produced from rice husk ash: Comparison of purification and processing methods. *Mater Res* 2017; 20: 512–518.
 47. Davidovits J. *Geopolymer chemistry and applications*. Saint-Quentin, France: Geopolymer Institute, 2015.
 48. Rahman AS and Radford DW. Evaluation of the geopolymer/nanofiber interfacial bond strength and their effects on Mode-I fracture toughness of geopolymer matrix at high temperature. *Compos Interf* 2017; 24: 817–831.